Probing General Relativity in galactic scales at z ~ 0.3

Published in MNRAS - arXiv:2212.08463v2

Carlos Roberto de Melo[†], Cristina Furlanetto, Ana Chies Santos
Instituto de Física, Universidade Federal do Rio Grande do Sul, Brazil
[†] carlos.melo@ufrgs.br

see the full work

Introduction

General Relativity (GR) has undergone numerous tests over the years, and has proven to be the most successful theory of gravity[1], especially in light of precise tests in the Solar System and the Milky Way. However, despite its successes, some unresolved tensions remain, such as the so-called Hubble tension and the detection of dark matter and energy. To address these tensions, various modified theories of gravity have been proposed[2], and extragalactic tests of GR have been performed to establish constraints on both GR and these alternative theories. In the weak field regime, a common method to test gravity is to use linearized gravity, where the gravitational slip parameter[3] η is defined as the ratio of two scalar potentials that appear in the linear perturbed FLWR metric. The first potential, the Newtonian potential Φ, acts on massive and non-relativistic particles, while the second potential, the curvature potential Ψ, is related to the curvature of space-time and is more important for the motion of relativistic and massless particles. Under the assumptions of GR and three additional conditions: (i) a vanishing anisotropic stress tensor; (ii) a well-defined Newtonian limit; and (iii) constancy of η under the relevant scales being studied, $\Phi \equiv \Psi$, and therefore $\eta = 1$. This approach has been used to test GR and alternative theories of gravity in various astrophysical and cosmological contexts[4,5,6,7]. Due to the nature of η, the motion of non-relativistic and relativistic particles can be differentially affected. This makes it possible to probe it by comparing the masses inferred by different tracers (e.g. cluster dynamics and gravitational lensing), which are sensitive to the different potentials of the same extragalactic object. To date, the most precise measurement of the slip parameter ($\eta = 0.97 \pm 0.09$) was achieved by Collett et al. (2018)[5] using strong gravitational lensing (SGL) and spatially resolved stellar kinematics of the lens galaxy for a system at $z_l = 0.035$. In this work, using ALMA, HST, and VLT/MUSE data, we probe η by simultaneously modelling lensing and dynamical masses in a self-consistent way, for a new system SDP.81 at intermediate redshift ($z_l = 0.299$) and therefore at much higher distante.

Gravitational Lensing

To probe η using SGL, we use high resolution ALMA observation[8,9] in the band 7 continuum of the SDP.81 system (Fig. 1). In SGL, the positions of the multiple images formed are related to the amount of mass that is deforming the space-time in that region. Thus, we can use these positions as constraints for the lensing model to estimate the mass distribution of the lensing object.

Stellar Kinematics

We can also probe the mass of the lens object by measuring the kinematics of the stars in the lens galaxy. Spectroscopic observations can reveal how fast the stars are moving along the LOS. Once individual stars cannot be resolved in distant galaxies, the problem is approached statistically, by solving the Jeans Equations to describe the stellar motion of the lens galaxy and obtain a dynamic model. IFS observations from the VLT/MUSE provide the kinematic maps used for the dynamical modeling, which are fitted with **pPXF**[10] to obtain the velocity and velocity dispersion along the LOS in the wavelength range of 5000-7000Å. The root-mean-square velocity ($V_{rms}^2 = v^2 + \sigma^2$) is used as a constraint for the dynamical modeling and is shown in Figure 2.

Combined Modelling

We simultaneously model the SGL data and the kinematic data using a flexible and self-consistent mass profile parametrized by a sum of elliptical Gaussians (the MGE[11] approach), which allows us to decompose the mass profile into two components: (i) a stellar-mass component, obtained by deprojecting the observed lens surface brightness profile (obtained from the HST WFC/F160W observations); (ii) a dark matter halo, described by an NFW profile[12]. The lens modelling was performed using **PyAutoLens**[13], while the kinematics modelling was performed using **JAM**[14]. We built a joint likelihood and explore the parameter space using the Bayesian nested sampling code **dynesty**[15] to find the most probable model that reproduces both data simultaneously. To avoid problems with exploring the parameter space and reconstructing the source, we developed a pipeline that breaks the combined modelling into different phases. A schematic representation is shown below.

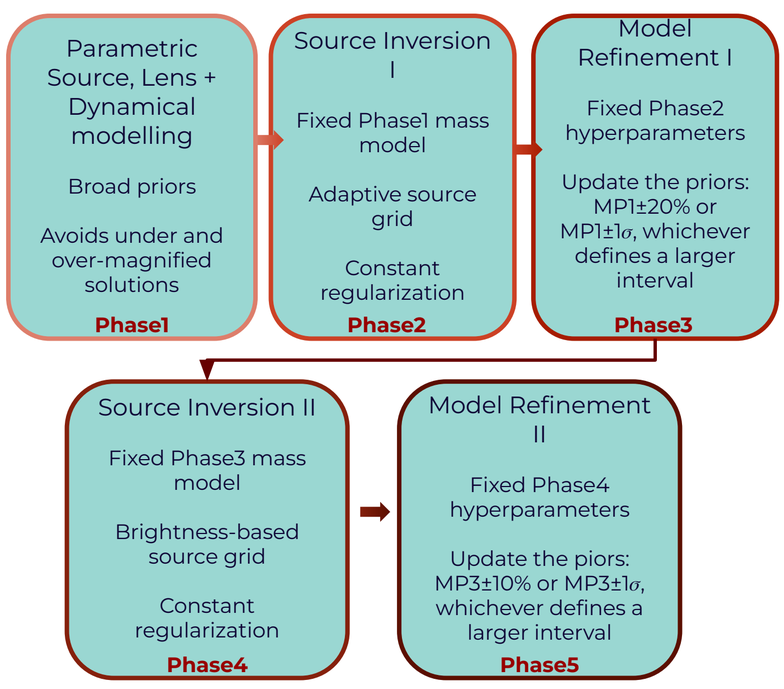

Results and Discussion

The fiducial model was obtained by fitting simultaneously both the observed lensing and kinematical data. Due to the complexity of the model adopted, we can derive different properties of the lens galaxy, and at the same time, reconstruct the source emission. The most probable lens model, the reconstructed source and dynamical model are shown in Figs. 1 and 2. We estimate the Einstein radius $R_{Ein} = 1.61''$, which agrees with previous studies[16,17]. The dark matter content represents ~35% of the total mass[18] within R_{Ein}. Finally, for the fiducial configuration, we infer $\eta = 1.14 \pm 0.03$ (stat), which is in tension with GR. Meanwhile, as demonstrated by previous works, systematic uncertainties are the main source of uncertainty on η.

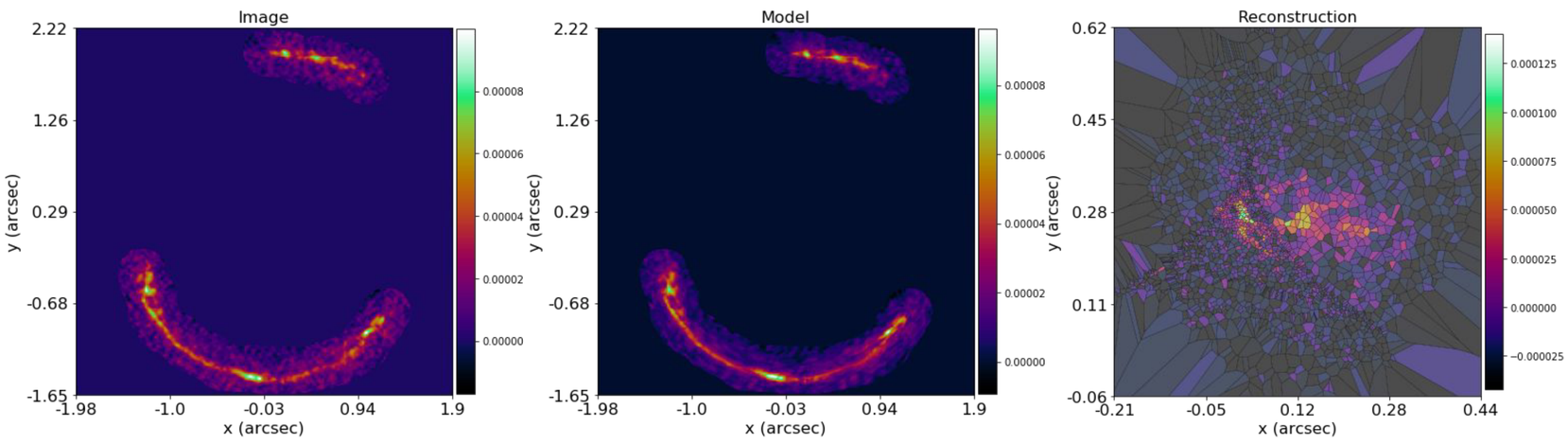

Figure 1 (Above): ALMA observations band 7 of SDP.81, most probable model and reconstructed source. All images are rotate by the galaxy position angle.

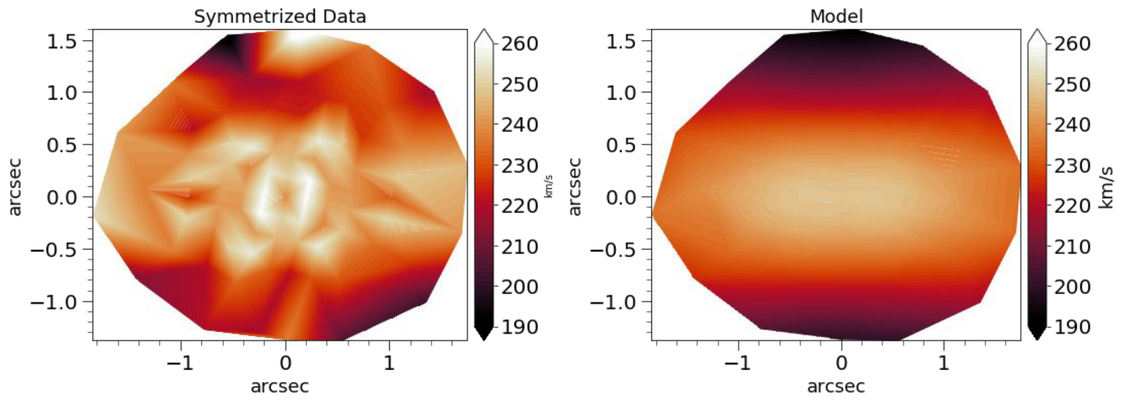

Figure 2: Root-mean-square velocity along the LOS, inferred by **pPXF** modelling and most probable model. The original spaxels are binned to a minimum signal-to-noise ratio of 25. The figures are linearly interpolated for better visualization, and rotated by the position angle

To better understand the accuracy of our measurements, we investigated potential sources of systematic error. We considered three factors that could impact our results: the choice of mass model, the assumed value of H_0, and the specific template used to derive the kinematical map. Then, we combine all these systematic uncertainties in quadrature to achieve the final result.

Impact of the choice of the mass profile	**0.017 (sys)**
Impact of Cosmology	**0.043 (sys)**
Impact of the choice of the stellar library	**0.190 (sys)**

Final Inference

$$\eta = 1.13^{+0.04}_{-0.03} \pm (0.20)^{\mathrm{sys}}$$

Conclusions

Despite the careful analysis of the uncertainties affecting the inference of the gravitational slip parameter, we have still **recovered GR within the uncertainties.** However, the issue of kinematical uncertainty remains a significant challenge, particularly if we aim to achieve percent-level precision in probing GR beyond the local Universe. Therefore, a more better characterization of these systematic uncertainties and possible biases in the modeling is crucial. In this context, hydrodynamical simulations like Illustris[22] can be used to help in identifying such biases and better comprehending the limitations and uncertainties related to the kinematical map. This could, for instance, aid in determining the number of kinematic measurements required to tightly constrain η at the percent-level.

References

Check out the full references in the QR code bellow

About me

Check out my interests and current project

Acknowledgements

CNPq
PPG FÍSICA UFRGS
Laboratório Nacionalde Computação Científica
CBPF

References

1. Will, C. M. (2018). Theory and Experiment in Gravitational Physics. In Cambridge University Press.
2. Ishak, M. (2019). Testing general relativity in cosmology. Living Rev. in Relativ., 22(1).
3. Cappellari, M. (2002). Efficient multi-Gaussian expansion of galaxies. MNRAS 333(2), 400–410.
4. Schwab, J., Bolton, A. S., & Rappaport, S. A. (2010). Galaxy-Scale Strong-Lensing Tests of Gravity and Geometric Cosmology: Constraints and Systematic Limitations. ApJ, 708(1), 750–757.
5. Collett et al. (2018). A precise extragalactic test of General Relativity. Science, 360(6395), 1342–1346.
6. Cao, S. et. al. (2017). Test of parametrized post-Newtonian gravity with galaxy-scale strong lensing systems. A.J. 835(1), 92.
7. Pizzuti, L. et. al. (2016). CLASH-VLT: Testing the nature of gravity with galaxy cluster mass profiles. J. Cosmol. Astropart., 2016(4).
8. Negrello et al. (2010). The Detection of a Population of Submillimeter-Bright, Strongly Lensed Galaxies. Science, 330(6005), 800–804.
9. Vlahakis et al. (2015). The 2014 alma long baseline campaign: Observations of the strongly lensed submillimeter galaxy hatlas J090311.6+003906 at z = 3.042. Astrophys. J. Lett., 808(1).
10. Cappellari, M. (2017). Improving the full spectrum fitting method: Accurate convolution with Gauss-Hermite functions. MNRAS, 466(1), 798–811.
11. Cappellari, M. (2002). Efficient multi-Gaussian expansion of galaxies. MNRAS 333(2), 400–410.
12. Navarro, J. F., Frenk, C. S., & White, S. D. M. (1997). A Universal Density Profile from Hierarchical Clustering. ApJ 490(2), 493–508.
13. Nightingale, J. W., Dye, S., & Massey, R. J. (2018). AutoLens: automated modeling of a strong lens's light, mass, and source. MNRAS, 478(4), 4738–4784.
14. Cappellari, M. (2008). Measuring the inclination and mass-to-light ratio of axisymmetric galaxies via anisotropic Jeans models of stellar kinematics. MNRAS, 390(1), 71–86.
15. Speagle, J. S. (2020). dynesty: a dynamic nested sampling package for estimating Bayesian posteriors and evidences. MNRAS, 493(3), 3132–3158.
16. Dye, S. et. al. (2015). Revealing the complex nature of the strong gravitationally lensed system H-ATLAS J090311.6+003906 using ALMA. MNRAS, 452(3), 2258–2268.
17. Vlahakis, C. et. al. (2015). The 2014 alma long baseline campaign: Observations of the strongly lensed submillimeter galaxy hatlas J090311.6+003906 at z = 3.042. ApJL, 808(1).
18. Sonnenfeld, A. et. al. (2015). THE SL2S GALAXY-SCALE LENS SAMPLE. V. DARK MATTER HALOS AND STELLAR IMF OF MASSIVE EARLY-TYPE GALAXIES OUT TO REDSHIFT 0.8. ApJ, 800(2), 94.
19. Planck Collaboration (2016). Planck 2015 results. A&A, 594, A13.
20. Shajib, A. et. al. (2020). STRIDES: a 3.9 per cent measurement of the Hubble constant from the strong lens system DES J0408−5354. MNRAS, 494(4), 6072–6102.
21. Millon, M. et. al. (2020). TDCOSMO. A&A, 639, A101.
22. https://www.tng-project.org/